Quaternary Geochronology 82 (2024) 101542

Contents lists available at ScienceDirect

Quaternary Geochronology

journal homepage: www.elsevier.com/locate/quageo

Research paper

Probing sediment burial age, provenance and geomorphic processes in dryland dunes and lake shorelines using portable luminescence data

A. Stone[a,*], M.D. Bateman[b], D. Sanderson[c], S.L. Burrough[d], R. Cutts[a], A. Cresswell[c]

[a] Department of Geography, The University of Manchester, M13 9PL, UK
[b] Department of Geography, University of Sheffield, Winter St., Sheffield, S10 2TN, UK
[c] Scottish Universities Environmental Research Centre, Rankine Avenue, Scottish Enterprise Technology Park, East Kilbride, G75 0QF, UK
[d] School of Geography and the Environment, University of Oxford, South Parks Road, Oxford, OX1 3QY, UK

ARTICLE INFO

Keywords:
OSL dating
Portable luminescence reader (POSL or port-OSL)
Rapid age assessment
Drylands
Quaternary environments
Dunes
lake shorelines
Provenance
Geomorphic processes

ABSTRACT

Luminescence signals from portable optically-stimulated luminescence readers (POSL or port-OSL) can provide expedient insights into sample relative age, and under certain conditions can be simplistically calibrated against existing luminescence chronologies to provide first-order estimates of burial age. This is most straightforward in simple sedimentary systems where samples share a common provenance and geomorphic process history. The spatially extensive southern African dune and palaeolake shoreline luminescence database, for which hundreds of non-light exposed bulk sediments are available, offers a valuable test case to examine the conditions under which POSL-bulk sediment calibration approaches are feasible. To do this we combine measurements of inherent luminescence sensitivity of bulk sediment (BSS) with analysis of sedimentary composition (petrology and presence of calcium carbonate) and texture. We show that BSS, along with POSL IRSL:BSL ratios and petrological data, account for region-to-region variations, whilst internal variability (scatter) within the lake shorelines dataset relates to variations in BSS and sediment texture. At the scale of southern African subcontinent drylands, we see that provenance and geomorphological process history influence sample mineralogical composition and POSL signal characteristic, including BSS.

1. Introduction

Portable luminescence readers are an approach developed to ‘speed up’ the time- and resource-intensive laboratory luminescence dating process (Sanderson and Murphy, 2010; Munyikwa et al., 2021). Other laboratory-based approaches include: (i) luminescence profiling using bulk or partially-processed sediment with laboratory-bound readers (e.g. Sanderson et al., 2001, 2003; Burbidge et al., 2007); (ii) simplified chemical preparation procedures to provide range-finder equivalent doses (D_e) and ages (e.g. Roberts et al., 2009; Durcan et al., 2010; Leighton and Bailey, 2015), and (iii) creating a standardised growth curve (SGC) to reduce analytical reader time (Roberts and Duller, 2004; Telfer et al., 2008). Portable optically stimulated luminescence (POSL, or port-OSL) analysis of bulk sediment samples is well-suited for expedient luminescence profiling with the additional benefit of being applicable in the field during sampling or back in the laboratory without any sample preparation steps (e.g. Sanderson and Murphy, 2010; Stone et al., 2015; Bateman et al., 2018). Refinements of POSL capabilities have been attempted, including: (1) rapid D_e estimation using POSL IRSL (infra-red stimulated luminescence) signals (targeting polyminerals) combined with SGCs produced from laboratory-irradiated bulk samples (Munyikwa and Brown, 2014) and (2) a calibration approach for approximating sample ages from bulk sediment POSL BSL (blue-stimulated luminescence) signals that utilises samples with existing age estimates (using standard quartz OSL protocols) for a regression model (Stone et al., 2015, 2019). The latter approach was developed for southern African dune samples and has subsequently yielded favourable results for archaeological terraces in the Judean Highlands, Israel (Porat et al., 2019), palaeo-wetlands in Las Vegas Valley, Nevada, U.S.A. (Gray et al., 2018) and Thar desert dunes, India (Nitundil et al., 2023).

Southern Africa (Fig. 1) is a valuable test case to explore the conditions under which rapid approximate age assessment using POSL calibration approaches is feasible for dryland geomorphological palaeoenvironmental archives. Dunes and lake shorelines are the key archives in drylands because biological proxies are poorly preserved, and also particularly in regions lacking carbonate bedrock to facilitate

* Corresponding author.
E-mail address: abi.stone@manchester.ac.uk (A. Stone).

https://doi.org/10.1016/j.quageo.2024.101542
Received 6 November 2023; Received in revised form 3 May 2024; Accepted 7 May 2024
Available online 10 May 2024

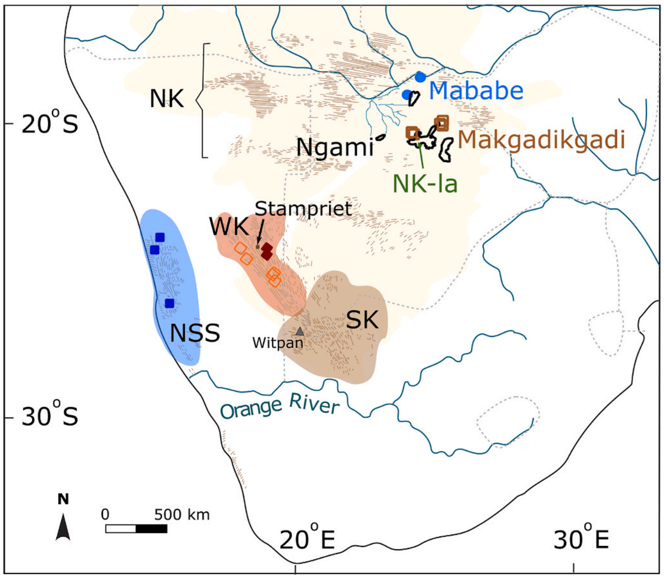

Fig. 1. Map of southern Africa, showing position of: (i) dunefields, Namib Sand Sea (NSS) (blue, where sample locations are blue squares), southern Kalahari (SK) (brown, where sample locations are grey triangle), western Kalahari (WK) (orange-red, where samples locations west of Stampriet are open orange diamonds and sample locations east of Stampriet are closed, dark red diamonds), and the pan surface landforms in the northern Kalahari (NK) (green crosses are used for these in Fig. 3) (light yellow depicts extent of Kalahari group sediments); and (ii) palaeolake locations (in Figs. 2 and 3 Ngami samples have open black circles, Mababe samples have light-blue solid circles and Makgadikgadi sample have open brown squares). Detailed maps of each of the shorelines systems for each of the palaeolakes is given in Supp. Info. 1).

deposition of speleothems and tufa, or without rock-shelters to host hyrax middens (Thomas and Burrough, 2012; Stone, 2021). The utility of dunes and lake shorelines as palaeoenvironmental proxies relies on our ability to provide chronologies for their accumulation and being able to do this at the landscape-scale (Stone and Fenn, 2022), which is extremely time consuming, and resource intensive based on laboratory-dating alone. This makes POSL calibration approaches an exciting prospect, where simple age-signal relationships can be established (e.g. Stone et al., 2019; Nitundil et al., 2023). Exploring the POSL calibration approach for multiple dunefields in southern Africa revealed a need for region-specific regression curves (Stone et al., 2019), which is not unexpected given the unique luminescence growth curves, and site-specific SGCs required to calibrate estimates of the natural dose received by a sample into equivalent laboratory dose (e.g. Telfer et al. (2008) and Yang et al. (2011) for dryland dunes), and noting that these use targeted minerals and particle sizes. In its simplest form, POSL of bulk (unprocessed) sediment samples measures mixed signals (quartz, feldspar, and other sensitive minerals) across a range of particle sizes, without accounting for variations in inherent luminescence sensitivity of the bulk sediment (see an excellent discussion of POSL drawbacks in Munyikwa et al. (2021)). This means that expedient estimates of approximate sample age using bulk sediment POSL will be most straightforward for groups of samples exhibiting a similar luminescence behaviour, and this requires a simple sedimentary system. Such a system has a common sedimentary provenance and geomorphic process history, which in turn controls key sample characteristics, such as mineralogical composition, particle-size distribution, and inherent luminescence sensitivity of minerals within the bulk sediment. Transport mode is a control on the completeness of signal bleaching prior to burial. Consequently, interpolation of chronologies within a simple sedimentary system is far safer than extrapolating beyond the bounds of that system. It is important to develop frameworks to support the age to POSL signal relationships and incorporate checks to establish the limits of application.

This study aims to test the use of POSL signals for rapid age assessment (POSL calibration) in lake shoreline sediments as compared to those established (and refined here) for dunes, and to evaluate the bounds of each sedimentary system per region. In doing so we explore how to use POSL signals to better understand age, provenance and geomorphic processes. We use an extensive dataset of samples ($n = 135$) from the megalake Makgadikgadi system (Lake Ngami, the Mababe Depression with Chobe back-flooding zone and Lake Makgadikgadi) of northern Botswana in the northern Kalahari (Burrough et al., 2009a,b), and $n = 79$ dune samples, reanalysed here. In addition, we provide the first measurements of inherent luminescence sensitivity of bulk sediment (from here on, abbreviated to BSS for bulk sediment sensitivity) for a subset of dune and lake shoreline samples to establish whether this is a key determinant of region-specific POSL calibration curves. This study also explores how the combination of POSL signal characteristics, BSS and sediment texture data may be used to cast some light on geomorphic processes, including sediment provenance and sediment transport pathways, as part of a reflexive geomorphological approach.

2. Methods

This study utilises available non-light exposed bulk samples for which there are published quartz OSL age estimates. For POSL calibration, we use 5 cm diameter Petri dishes with an approximate monolayer of grains in a POSL sequence of 15 s dark count, 60 s IRSL estimation (LEDs passed through an RG780 long pass filter), 15 s dark count (includes phosphorescence), 60 s post-IR OSL (LEDS passed through a CG420 long pass filter), which we refer to here as BSL (blue-stimulated luminescence), and 15 s dark count (includes phosphorescence), where all emitted signals are filtered through UG11 filters. For data analysis we use the widely applied approach of Sanderson and Murphy (2010), which uses the total signals over 60 s (minus the dark counts, inclusive of phosphorescence) for IRSL and BSL. All available bulk samples from lake shorelines of Ngami (70 samples from Burrough et al. (2007)), Mababe (29 samples from Burrough and Thomas (2008)) and Makgadikgadi (36 samples from Burrough et al. (2009)) were measured. Note that the POSL measurement protocol and data analysis employed here are different from the method employed in Stone et al. (2015, 2019), and we make this switch to facilitate data comparability with other sites across the literature. This required us to re-measure dune samples from the southern Kalahari (SK), western Kalahari (WK) and the Namib (NSS). It is important to highlight that we have a different sample dataset (in terms of n) for each dune region than in Stone et al. (2019), owing to the availability of material: (i) 22 of the initial 64 for SK, (ii) 32 of the initial 36 for WK west, (iii) 2 of the initial 3 for WK east of Stampriet, and (iv) 5 of the initial 24 for NSS, but with 18 different/additional NSS samples found in storage and measured (bold and starred in column F, Supp. Info. 3). This may influence the calibration curves produced here in addition to employing the revised POSL protocol. Unfortunately, there was no non-light exposed bulk for the landforms on the surface of Makgadikgadi (note an NK-la (the -la stands for lakebed landforms) compared to -Ba (for barchans) in Stone et al. (2019), is made here to reflect the debated origin of these landforms). However, we use light-exposed material for the second aspect of this study.

Bulk sediment sensitivity (BSS) is a measure of the inherent luminescence sensitivity of a bulk sample to a known radiation dose and can be assessed after zeroing the signal and laboratory irradiating it. Analyses were undertaken at the Scottish Universities Environmental Research Centre (SUERC) for a selection of three paired sub-samples for each dunefield region (NSS, SK, WK west and WK east), a slightly larger selection of samples within each palaeolake shoreline system (8 samples from Ngami, 11 samples from Mababe and 9 samples from Makgadikgadi, with some paired sub-samples), and three paired subsamples from NK-la (Supp. Info. 4). This requires sediment to be mounted on 3 cm diameter metal planchets using silicone spray, rather than in the plastic petri dishes used above, to allow sample heating. Small variations in sample mass do not drive variations in BSS (Supp. Info. 4, Fig S4.5). No non-light exposed bulk was available for Mababe shoreline samples or for NK-la sediments. For all other samples, natural luminescence signals were first measured using POSL for each planchet before heating to 300–350 °C for 5 min (following a 3–4 min temperature ramp up, as measured using a thermocouple) to bleach any remaining luminescence signal. Whilst we recognise that heating can induce changes in luminescence behaviour, this was a pragmatic choice given the constraint of time and the challenge of fully bleaching sufficient sediment volume using light exposure. Treating all samples in an identical way facilitates a meaningful comparison for these BSS experiments. 4 Gy of laboratory irradiation, using a 4 cm^2, ^{90}Sr source irradiator (Sanderson and Chambers, 1985), set up with a 7.45 cm working distance, giving approximately 200 mGy per minute irradiation to the 3 cm planchets, as described by Francoz (2023). This was chosen as a compromise between irradiation time (~20 min) and producing large enough POSL luminescence signal for counting statistics. We also use petrological data (quartz/feldspar/lithics and heavy minerals >2.9 g/cm^3) for sediment across southern Africa from Garzanti et al. (2012), Stone et al. (2019) and Garzanti et al. (2022) (see those papers for relevant methodologies).

3. Results

3.1. Calibrations using regressions of portable reader signals against luminescence ages

The regression lines of blue POSL against quartz age for the ***dune samples*** (re)measured in this study (Fig. 2A) are different to those in Stone et al. (2019), as expected, driven both by moving to the standardised POSL protocol and analyses approach and measuring a different set of samples. We gain the advantage of a dataset that is readily comparable to other datasets in the literature. Most striking, is the reduction in the gradient of the NSS line relative to the other regions – now positioned to the right of SK (formerly to the left). Supp. Info. 3 includes a comparison of regressions for completeness. NAM07/3/1 (used in the original calibration) has a quartz age close to saturation ($D_e > 2 \times D_0$, which Wintle and Murray (2006) guide as an upper limit), as do two other available dune samples (NAM07/3/3 and 3/5) (Supp. Info. 3). The parsimonious choice is to exclude them from the calibration in Fig. 2. We now have two ages for the Narabeb dune sediment material established using $pIRIR_{225}$ feldspar dating protocols (e.g. Thomsen et al., 2012), which offer us some age control for the upper age-range of the calibration (Stone et al., 2024). We note that the NSS calibration remains poorly constrained, and a greater number of the >80–90 ka (saturated quartz) sediment at Narabeb and new locations in the NSS are needed in future studies. Going forward, further application of pIRIR dating protocols will be useful to extend the calibration approaches above the range of quartz signal saturation across a range of southern African sites and sedimentary settings.

Fig. 2B shows that ***lake shoreline samples*** have brighter POSL BSL for their age compared to western (WK) and southern (SK) Kalahari dunes, and slightly brighter than NSS dunes. The shoreline datasets contain more scatter, and we look for any within-palaeolake system geographic patterns in Supp. Info. 3. No consistent geographical trends are seen for: (i) northern, southern and western shorelines at Lake Ngami, or for lakebed sediments (Fig. S3.2B), (ii) Lake Mababe Magikwe Ridge versus the Parakarungi ridge in the Chobe back-flooding zone (Fig. S3.2C); and (iii) Lake Makgadikgadi Gidikwe Ridge (south) and the northern ridge and spit near Nata (Fig. S3.2D). However, the two oldest Makgadikgadi samples stand out having much dimmer POSL for their age (Fig. 3.2C), and it is prudent to suggest these quartz ages >250 ka could be close to signal saturation. Another observation is that many of the samples for which calcrete was noted in the field (Burrough et al., 2007, 2009) have brighter POSL relative to other samples, particularly for Lakes Ngami and Makgadikgadi (Fig. S3. Fig2B,D).

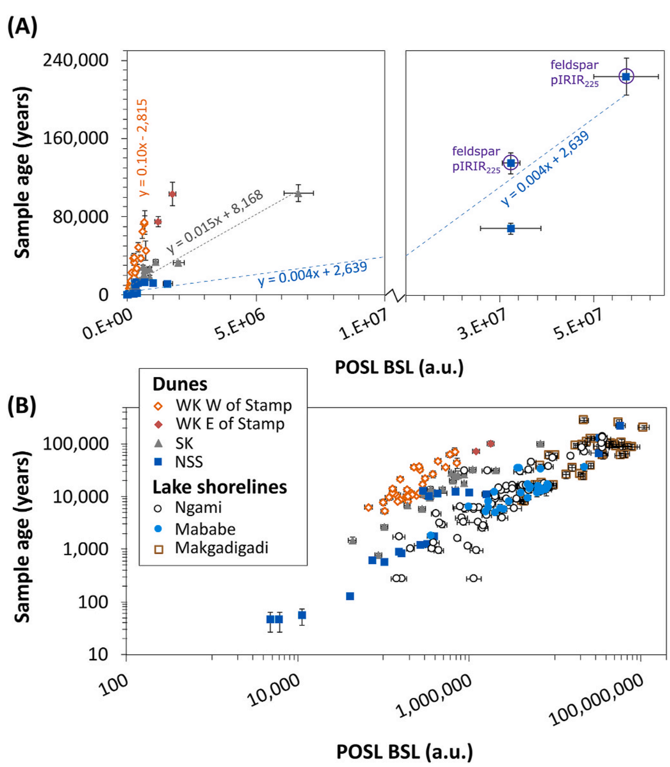

Fig. 2. Sample ages regressed against POSL (post-IR) BSL signals: (A) dune samples* using linear fit (please NOTE the break in the x axis and change in axis scale to depict the brightest and oldest of the NSS samples) and (B) dune samples* and lake shoreline samples on a log-log plot (* NOTE re-measured and analysed compared to Stone et al. (2019) dataset). (see Supp. Info. 3 for an exploration of the lake shoreline dataset).

3.2. Bulk sediment luminescence sensitivity (BSS) tests

The 4Gy BSS tests show that each ***dune region*** has a distinct bulk sediment luminescence (Fig. 3A), indicating that BSS is indeed an important factor driving the regional patterns within POSL to age calibrations (Fig. 2A). The NSS is the brightest (most sensitive) in both BSL and IRSL. The BSL sensitivity varies over one order of magnitude between the NSS and the Kalahari, and within the Kalahari the SK and WK (east of Stampriet) are of a similar magnitude, whilst WK (west) is about half as sensitive. The IRSL sensitivity varies over two orders of magnitude between the NSS and the Kalahari with the second brightest response in the SK and very dim responses for both parts of the WK (Fig. 3A–Table 1). The regional patterns in the ratio of IRSL to BSL signals for sensitivity responses (BSS) are consistent with the natural signals, indicating a similar response of the bulk sediment to dosing in nature and dosing in the laboratory (Fig. 3B for the subset of samples used for BSS tests on planchets and Fig. 3C for the full dataset measured in POSL 'standard' Petri dishes) (Table 1 shows averages per dune region and full data in Supp. Info. 3&4). ***Lake shoreline*** sediments for all three lakes are highly sensitive in BSL but amongst the least sensitive in IRSL (Fig. 3A). The low sensitivity in IRSL is mirrored by low natural IRSL signals (Fig. 3B and C), and IRSL:BSL ratios approaching zero (Table 1 shows regional averages, with full data in Supp. Info. 3&4). The three lake shorelines do not have discrete ranges in BSL sensitivity, with overlapping ranges, although the brightest (most sensitive) samples are from the Makgadikgadi group (Fig. 3A). The ***NK-landforms*** have very dim IRSL sensitivity, and a highly variable BSL sensitivity (3.8×10^4 to 5.4×10^5) (Fig. 3A–Table 1). Given their location on the Ntwetwe Pan region of the floor of lake Makgadikgadi, it is notable the BSL sensitivities of NK-la do not define the same range as Makgadikgadi shorelines.

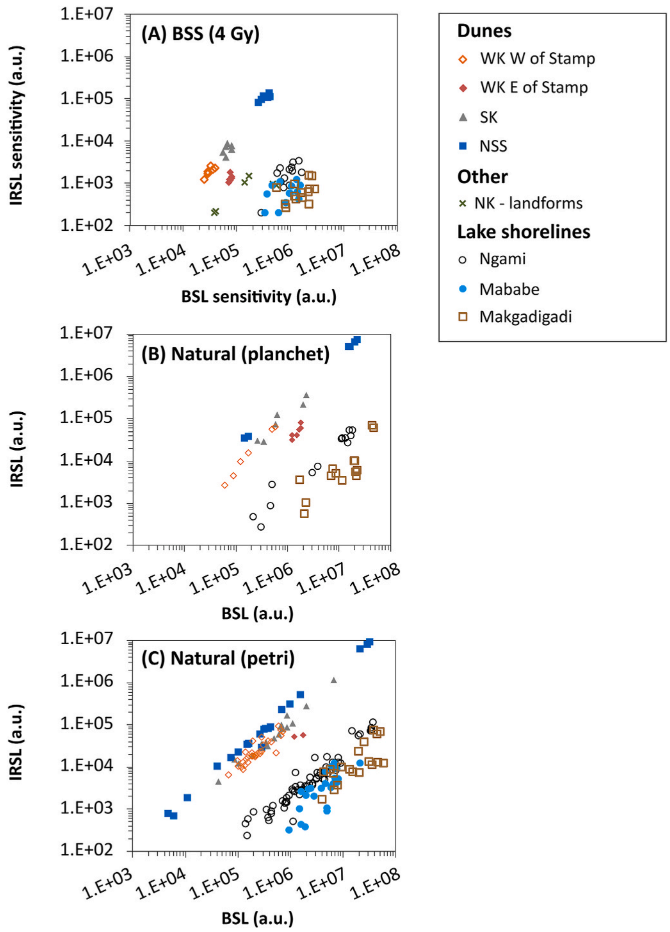

Fig. 3. (A) Post-IRSL BSL and IRSL bulk sediment (BSS) response to a 4 Gy dose for subsamples from the four dune regions, and three lake shoreline regions. Natural signals are plotted for comparison, where **(B)** is on the planchets prior to heating/bleaching, and **(C)** is from the larger petri-dish dataset.

4. Discussion

4.1. Regional patterns in bulk sediment luminescence sensitivity

Across the entire dataset there are: (i) 2 orders of magnitude variation in IRSL sensitivity, which fall into three groups (by net counts): high (NSS, 0.8-1 x 10^5), low (SK 4-9 x 10^3) and very low (all the other regions with ≤2.5 x10^3); and (ii) 3 orders of magnitude variation in BSL, where lake shorelines from NK are most sensitive (0.3-3 x 10^6 total counts, with most sensitive samples within the Makgadikgadi shoreline group), then the NSS (2-4 x 10^5), overlapping with the upper range for NK-la (0.4-5 x 10^5), then WK (east) and SK (7-8 x 10^4 and 5-8 x 10^4, respectively), and then WK (west) (2-4 x 10^4) (Table 1 summary, Supp. Info. 4 for data in full). A number of factors can drive these differences, including sediment texture and petrological composition.

One of the factors is the combination of minerals that is present in any bulk sediment sample. This includes the percentages of quartz (Q) and feldspar (F) in our sample and the presence of any other luminescent minerals. POSL IRSL comes from F, rather than from Q (and may also come from other luminescent minerals), whilst BSL signal is likely to be dominated by Q but will also include any F response that was not zeroed from IRSL stimulation (plus any other luminescent minerals) (see Munyikwa and Brown, 2014). In addition, the inherent sensitivity of individual minerals varies spatially, as inherited from mineral formation processes and subsequent alteration during repeated samples of transport and burial. For example, for quartz, high temperature source rocks show higher OSL sensitivity (e.g. Sawakuchi et al., 2011), and an increased number of cycles of irradiation and light exposure in nature has been demonstrated to increase sensitivity (e.g. Pietsch et al., 2008; Zheng et al., 2009; Fitzsimmons, 2011; Sawakuchi et al., 2011; Lü et al., 2014), as does heating of sediment in wildfires (Rengers et al., 2017). Feldspar sensitivity is also variable, for example as recently reported by Fitzgerald et al. (2022) for 22 different feldspars using POSL.

Petrological data are available for dune sediment in the NSS, SW, WK (west), WK (east) and for sediment from the NK landforms on the Ntwetwe portion of Makgadikgadi pan (Garzanti et al., 2012, 2022; Stone et al., 2019) (Table 1). However, for the lake shoreline systems it is only available from nearby dune and river samples in the NK (Garzanti et al., 2022). Are variations in petrology sufficient to explain the trends in BSS? The highest IRSL sensitivity group (NSS) does have the highest overall percentages of feldspar (%F) and Q:F 3–4, and the very low-to-no IRSL signal group (NK) has the lowest (<1% F) and with a few exceptions Q:F (Table 1). The NSS contains feldspathoquartzose sands with a rich heavy mineral suite (Q:F 3–4), with much of the sand long-travelled from the Orange River, indicating much of the western NSS is a wind-displaced river delta (Garzanti et al., 2012; Stone et al., 2019). However, the small variations in %F within the rest of these data do not match relative trends in IRSL sensitivity. For BSL, whilst highest quartz percentage (%Q) are found for the highest sensitivity group (all lake shoreline sediments together) (91.5–100%), beyond this there is no consistent trend between %Q and BSL sensitivity. For example: (i) the second most sensitive BSL group (NSS) has the lowest %Q, and (ii) there are no %Q variations to explain why samples within the Makgadikgadi shoreline group contain the highest sensitivity of the lake groups. The BSL signals from NSS dunes may be influenced by feldspar (owing to non-zeroing in the IRSL). In addition, the rich heavy mineral (HM) suite within NSS sediments (7–8% concentration, compared to 0–2.5% for the SK, WK and NK), including zircon and garnet (Garzanti et al., 2012), warrants future investigation. See Schmidt et al. (2024) for a recent review of luminescnce dating of zircon. This investigation will require extraction of sufficient volumes of targeted HMs for POSL analysis.

It may not be surprising that mineralogical variation is an insufficient explanation for trends in BSS. We may just be observing variations in feldspar and quartz sensitivity across space in southern Africa, in line with observed variability in both feldspar and quartz sensitivity reported across the world (e.g. Pietsch et al., 2008; Zheng et al., 2009; Fitzsimmons, 2011; Sawakuchi et al., 2011; Lü et al., 2014; Rengers et al., 2017; Fitzgerald et al., 2022). Using this logic, the NSS may contain the most sensitive feldspar, whilst the NK contains the most sensitive quartz. In terms of the latter, Garzanti et al. (2022) argue that NK sands have undergone repeated sedimentary cycles between the fluvial and aeolian environments (as evidenced by near-pure quartzose sands with poor, or absent, HMs), and such cycling is a known to sensitise quartz (e.g. Pietsch et al., 2008). This contrasts with the quartz-rich feldspathoquartzose sands of the WK and SK that Garzanti et al. (2022) argue indicate first-cycle provenance from Damara Belt and Mesoproterozoic terranes. There is some “devil in the detail” within these broad observations. For example, what drives the variability/heterogeneity within each lake shoreline sediment group? We can note that the highest BSS comes from samples within in the Makgadikgadi group, which is furthest ‘downstream’ in the Okavango delta and this trend matches observations of increased sensitivity downstream in individual river systems (e.g. Pietsch et al., 2008).

In terms of sediment texture (Table 1, and Supp. Info. 4 for data per individual sample), we observe that dune sand sediments are relatively homogenous within and across dune regions (moderately to moderately-well sorted medium sand, sometimes fine sand) and that the small variations in sorting show no correlation with BSS (Fig. S5. Fig. 1A). In contrast to the dunes, sediments in the NK-landforms and lake shorelines vary in their degree of sorting. For NK-la there is a strong negative correlation between sorting and BSS, whilst for Ngami, Mababe and Makgadikgadi shorelines there is only a weak negative correlation (Fig. S5. Fig. 1C). Weak negative correlations are seen between silt

Table 1
Summary of POSL data for luminescence sensitivity tests on bulk sediment (BSS) undertaken on a subset of samples, POSL for the larger data for natural signals measured in petri dishes, alongside summary petrological data for each region.

	BSS (4 Gy dose) planchets				Natural		Petrology						
Sample	n	IRSL ± s.d. net counts	BSL ± s.d. net counts	IRSL: BSL (range)	n	IRSL: BSL (range)	ID	Q (%)	Plag F (%)	KF (%)	L (%)	HM (%)	Q:F
Dunes													
NSS	6	107914 ± 18793	338315 ± 65271	0.32 (0.27–0.37)	25	0.23 (0.11–0.94)	NAM07/4	70.0	9.7	12.8	0.5	7.0	3
							NAM13/6	71.1	7.2	12.7	1.0	8.0	4
SK	6	6554 ± 1654	66760 ± 9808	0.10 (0.06–0.13)	22	0.12 (0.08–0.20)	Bokspit	87.8	1.2	8.0	2.2	0.9	10
							KAL04/8	85.9	2.2	7.5	4.1	0.3	9
WK (W)	6	1939 ± 486	31038 ± 5430	0.06 (0.05–0.08))	32	0.10 (0.04–0.21)	KAL06/1	81.6	1.9	15.9	0.0	0.6	5
							KAL06/2	84.7	2.3	12.1	0.3	0.6	6
							KAL06/4	82.6	0.8	15.4	0.6	0.6	5
							KAL11/2	81.6	1.9	14.7	0.6	1.3	5
WK (E)	6	1313 ± 252	74971 ± 4171	0.02 (0.02–0.02)	2	0.04 (0.03, 0.04)	KAL06/6/1	89.1	0.6	8.4	1.4	0.6	10
							KAL06/6/3	88.4	0.3	8.3	0.0	2.5	10
							KAL11/3	87.0	0.6	11.9	0.6	0.0	7
Shorelines of the NK													
Ngami	13	1734 ± 897	925522 ± 368350	0.0019 (0.0007–0.0035)	70	0.0020 (0.0004–0.0055)	Toteng[d]	99.1	0.6	0.0	0.9	0.0	163
							Konde[d]	98.7	0.0	0.0	1.3	0.0	∞
							Toteng[r]	99.4	0.0	0.3	0.0	0.3	325
							Thaoge[r]	100	0.0	0.0	0.0	0.0	∞
Mababe	13	1103 ± 1745	923309 ± 419806	0.00008 (0.0003–0.0019)	29	0.00009 (0.0002–0.0035)	Chobe[r]	99.4	0.3	0.0	0.0	0.3	354
Makgadi-kgadi	14	588 ± 287	1658977 ± 714352	0.0005 (0.0001–0.0014)	36	0.00007 (0.0002–0.0019)	Nata[d]	91.5	4.1	4.5	0.0	0.0	11
							Damatsha[d]	92.9	0.6	6.3	0.0	0.3	14
							Boteti[r]	98.3	0.6	0.6	0.6	0.0	88
Other													
NK-la	6	1313 ± 252	230968 ± 216382	0.0051 (0.0017–0.0087)	NA	NA	Ntwete	94.5	0.3	1.5	2.5	1.2	52

[d] These data are for the nearest linear dunes in the northern Kalahari (NK) rather than the lake shorelines themselves. Toteng is 10 km east of Ngami, Konde is ~60 km northwest of Ngami. Nata is ~5 km from the ridge north of Nata (MAK06/1) and ~10 km north of the spit near Nata (MAK06/3) at Makgadikgadi, Damatsha is ~130 km southwest of the Gidikwe Ridge (at southern end of) Makgadigadi.

[r] These data are for river systems in the NK close to the lakes rather than the lake shorelines themselves. Toteng is ~10 km east of Ngami, Thaoge is ~40 km northwest of Ngami. Chobe is ~80 km northwest of Mababe Depression (Magikwe Ridge) and ~10 km east of the Chobe backflood samples at Parakarungu (MAB06/5-2 and 5-3). Botetu is ~90 km northwest of Makgadikgadi.

percentage and BSS (Fig. S5. Fig. 2D). Note that we only consider BSL BSS owing to very low IRSL signals in the quartz-rich sediments in our dataset. A detailed study of BSS per isolated grain-size fraction could help cast light on these tentative trends, however we lack sufficient volumes of existing bulk sediment to undertake such analysis, and untangling particle size and mineralogy would require yet greater volumes of sediment.

4.2. Sources of heterogeneity within lake shore sediments

Noting that simple sedimentary systems are more likely to show age-dependent POSL signals, there are several observed sources of heterogeneity in the lake shoreline sediments that drive scatter in attempted POSL age-calibrations, namely: (i) the presence of calcrete/carbonate in some samples, (ii) the observed range in BSL BSS (sensitivity) (Fig. 3A), and (iii) variability in particle size distribution between samples. To test the first, we took a subset (n = 8) of samples reported to contain calcrete (Burrough and Thomas, 2008; Burrough et al., 2007, 2009) and examined them closely in the luminescence laboratory. We then gently removed any white flecks and small concretions (assumed to be the calcrete/calcium carbonate) and measured triplicate subsamples for POSL to compare against the original POSL data. Supp. Info. 6 shows a 15–35% (mean 23%) lower BSL signal for subsamples where the material removed. In the spirit of using POSL as a simple field, or laboratory screening, tool we simply highlight this observation and encourage fellow practitioners to at least make a visual assessment of their samples and consider whether variations in colour, appearance and texture are potential explanatory factors for the POSL signals observed. It would be productive for a future study to explore what might drive a POSL BSL response in calcium carbonate, this requires sufficient volumes of the calcrete/calcium carbonate to work with. We can note that it cannot be the red (~600 nm) emission in calcite (e.g. Medlin, 1964 ; Carmichael et al., 1994) as POSL measures near-UV emission wavelengths (~250–400 nm). Calderon et al. (1984) observed other calcite TL peaks (~80–120 °C) ~380 nm but did not identify a process responsible for this peak.

For natural/burial dose POSL signals we explored the influence of sediment textural variability (and environmental dose rate as an additional variable) on those signals using a redundancy analysis (RDA) ordination approach (Fig. 4). In this approach, the POSL BSL signal is treated as the 'response' variable and sediment textural data as explanatory variables. This shows that sediment texture parameters along with environmental dose rate data may explain 34% of the total variation in natural signals. This suggests a significant role for other factors, which will include inherent sensitivity (as explored in our BSS experiments on a subset of samples) and the presence of calcium carbonate (note that having only present or absent categories for calcium carbonate means it could not be included into the RDA). Whilst it was not feasible to measure BSS response for 129 lake shoreline sediment samples to include in the RDA, our existing BSS dataset reveals that all three lake systems contain heterogeneity in inherent luminescence sensitivity between samples (also observed for the lakebed landform (NK-la)) sediments (Fig. 3A). We can observe that the fluvial systems that feed Makgadikgadi system drain a large spatial area up to the Angolan highlands, which when combined with wind-derived sediment from the NK dunefields, means that sediment available to build lake shorelines comes from a wide geographic area.

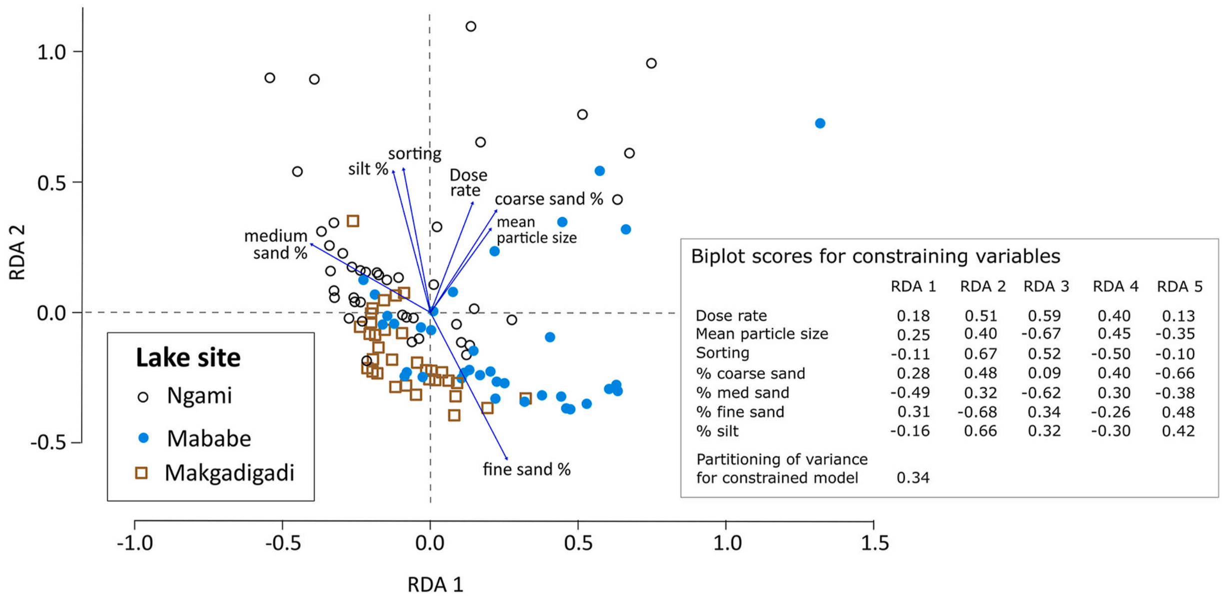

Fig. 4. Redundancy analysis (RDA) ordination plot for the POSL BSL signals for the lake shoreline sediments, also showing the biplot scores for the constraining variables for which we have discrete data (note for calcium carbonate content we only have present/absent categories, and only a small subset of samples have bulk sediment sensitivity (BSS) data).

4.3. POSL signals and an interpretive scheme

We have shown that POSL signals are influenced by sediment characteristics, including inherent luminescence sensitivity of bulk sediment (BSS) and sediment composition. In terms of composition, variations in minerology (e.g. Q:F ratios, presence of calcrete/calcium carbonate and perhaps luminescent heavy minerals) has some influence, as well as variations in particle size distribution. In developing a framework within which to evaluate age-POSL signal relationships these are important factors, along with sediment colour. In our test case of southern African drylands, dunefield systems tend to be sufficiently homogenous to allow us to classify them as *simple sedimentary systems*, and these produce sensible "calibrations" of POSL signals from which to rapidly assess burial age (Fig. 2A). However, whenever a sedimentary system demonstrates heterogeneity in mineralogical composition, and/or luminescence sensitivity and/or particle size distribution, this calibration is less precise. This seems to be case for northern Kalahari lake shoreline systems, particularly Makgadikgadi and the lakebed landform on the Ntwetwe Pan portion of it (Fig. 2B, Supp. Info. 3). Investigating sediment characteristics alongside POSL data allows us to employ an approach to POSL (and OSL) signals that considers how these signals relate to geomorphological processes, including a sensitisation of luminescence signals with increased transport pathways and cycles. As part of this "reflexive approach", Supp. Info. Table 1 is our summary of suggestions about what POSL signal characteristics can tell us about our bulk sediments (what the various POSL signal characteristics can be considered proxies for) alongside the factors that complicate each proxy by also having an influence on the selected POSL characteristic. We encourage other practitioners to interrogate these observations for their sedimentary systems.

5. Conclusions

POSL (or port-OSL) readers are insightful tools for exploring sample relative age and casting additional light into sediment provenance and geomorphic processes, and southern African dryland dunefields and lake shorelines are an excellent test case for this, using available bulk sediment of samples for which luminescence ages have been calculated. We build regression models (a form of "calibration") using BSL POSL signals because some regions have very little (to no) feldspar, and we find that there are region-specific calibrations: Namib Sand Sea dunes, southern Kalahari dunes, western Kalahari dunes and northern Kalahari lake shoreline systems (Ngami, Mababe and Makgadikgadi). The relationship between portable reader signals and age are more scattered for the three lake shoreline systems measured, particularly for the Makgadikgadi system. Within southern African drylands the dunefields are simple sedimentary systems, whilst the lake shorelines are more complicated.

In exploring these regional patterns, we measured bulk sediment luminescence sensitivity (acronym BSS) for the first time, using a subset of samples within each region (applying a 4 Gy beta dose in the laboratory after bleaching). This also reveals discrete regional groupings for our simple dune sedimentary systems, where the Namib Sand Sea is the most sensitive, then southern Kalahari, then western Kalahari. The northern Kalahari lake shorelines sediments are as sensitive, or more sensitive than the Namib Sand Sea but compared to dune samples display a large (> order of magnitude) degree of scatter/variability as a group. The shoreline BSS values display a weak correlation with the degree of sediment sorting (and silt percentage). The BSS data for each region, alongside existing petrological data for each of our regions provides us with insights into sediment provenance and geomorphic process. Across southern Africa: (i) the weakest BSS is from the westernmost western Kalahari dunes and this region has quartz-rich feldspathoquartzose sands, which are thought to indicate first-cycle provenance from Damara Belt and Mesoproterozoic terranes; (ii) the highest BSS is for the lake shorelines of the northern Kalahari and this region is composed of much purer quartzose sands (often with no feldspar left and a very poor heavy mineral suite) thought to indicate repeated sedimentary cycling between the fluvial and aeolian environment, a process known to sensitise quartz and feldspar and (iii) the Namib Sand Sea dunes also have high BSS in BSL and in IRSL (unlike any of the Kalahari groups), and this region contains feldspathoquartzose sands with rich heavy mineral suite, including zircon and garnet, ultimately derived from the Orange River. Within the more scattered lake shoreline dataset we observe that the most sensitive BSS (BSL) comes from samples from Makgadikgadi, which is the most distal of the lake shoreline systems, where sediments will have undergone sensitisation during repeated sediment cycling. Overall, POSL signals are inherently complicated by virtue of measuring bulk sediment with mixed sediment composition and sediment texture, which requires us to reflect carefully on sedimentary data alongside POSL data. In the case of southern Africa, the level of complexity in POSL data is neatly matched by the complexity of the sedimentary system.

CRediT authorship contribution statement

A. Stone: Writing – review & editing, Writing – original draft, Visualization, Resources, Project administration, Methodology, Investigation, Funding acquisition, Formal analysis, Data curation, Conceptualization. **M.D. Bateman:** Writing – review & editing, Investigation. **D. Sanderson:** Writing – review & editing, Resources, Methodology, Investigation. **S.L. Burrough:** Resources. **R. Cutts:** Formal analysis. **A. Cresswell:** Resources.

Declaration of competing interest

The authors declare that they have no known competing financial interests or personal relationships that could have appeared to influence the work reported in this paper.

Data availability

Data will be made available on request.

Acknowledgements

This research utilised samples collected as part of other projects and the reader is directed toward the acknowledgement of those papers for information regarding the relevant research/collecting permits. A.S. thanks Will Fletcher for productive discussions about RDA statistics, Edo Garzanti and his colleagues at the Università Milano-Bicocca for their previous collaboration on sediment petrology, and LED conference attendees for stimulating discussions around POSL data.

Appendix A. Supplementary data

Supplementary data to this article can be found online at https://doi.org/10.1016/j.quageo.2024.101542.

References

Bateman, M.D., Rushby, G., Stein, S., Ashurst, R.A., Stevenson, D., Jones, J.M., Roland, G.W., 2018. Can sand dunes be used to study historic storm events? Earth Surf. Process. and Landf. 43, 779–790.
Burbidge, C.I., Sanderson, D.C.W., Housley, R.A., Allsworth Jones, P., 2007. Survey of Palaeolithic sites by luminescence profiling, a case study from Eastern Europe. Quat. Geochron. 2, 296–302.
Burrough, S.L., Thomas, D.S.G., 2008. Late quaternary lake-level fluctuations in the Mababe depression: middle Kalahari palaeolakes and the role of zambezi inflows. Quat. Res. 69, 388–403.
Burrough, S.L., Thomas, D.S.G., Shaw, P.A., Bailey, R.M., 2007. Multiphase quaternary highstands at Lake Ngami, Kalahari, northern Botswana. Palaeogeogr. Palaeoclimatol. Palaeoecol. 253, 280–299.
Burrough, S.L., Thomas, D.S.G., Bailey, R.M., 2009. Mega-Lake in the Kalahari: a late pleistocene record of the palaeolake Makgadigadi system. Quat. Sci. Rev. 28, 1392–1411.
Calderon, T., Aguilar, M., Jaque, F., Coy-yll, R., 1984. Thermoluminescence from natural calcites. J. Phys. C Solid State Phys. 17 (11), 2027–2038. https://doi.org/10.1088/0022-3719/17/11/021.
Carmichael, L.A., Sanderson, D.C.W., Riain, S.N., 1994. Themoluminescence measurement of calcite shells. Radiat. Meas. 23 (2–3), 455–463.
Durcan, J.A., Roberts, H.M., Duller, G.A.T., Alizai, A.H., 2010. Testing the use of range-finder OSL dating to inform field sampling and laboratory processing strategies. Quat. Geochron. 5, 86–90 le.
Fitzgerald, S., Sanderson, D.C.W., Cesswell, A.J., Marin, L., 2022. Using Infra-red stimulated luminescence and phototransferred thermoluminescence to investigate electron trapping and charge transport in feldspars. Radiat. Meas. 156, 106817. https://doi.org/10.1016/j.radmeas.2022.106817.
Fitzsimmons, K.E., 2011. An assessment of the luminescence sensitivity of Australian quartz with respect to sediment history. Geochronometria 38, 199–208.
Francoz, C., 2023. Saltmarsh Resilience in a Changing Climate: Geomorphological and Biological Processes in Natural and Managed Salt Marshes in the Northeast of Scotland. University of Glasgow. PhD thesis.
Garzanti, E., Andò, S., Vezzoli, G., Lustrino, M., Boni, M., Vermeesch, P., 2012. Petrology of the Namib Sand Sea: long-distance transport and compositional variability in the wind-displaced orange delta. Earth Sci. Rev. 112, 173–189.
Garzanti, E., Pastore, G., Stone, A., Vainer, D., Vermeesch, P., Resentini, A., 2022. Provenance of Kalahari Sand: paleoweathering and recycling in a linked fluvial-aeolian system. Earth Sci. Rev. 224, 103867.
Gray, H.J., Mahan, S.A., Springer, K.B., Pigati, J.S., 2018. Examining the relationship between portable luminescence reader measurements and depositional ages of paleowetland sediments, Las Vegas Valley, Nevada. Quat. Geochron. 48, 80–90.
Leighton, C.L., Bailey, R.M., 2015. Investigating the potential of HCl-only treated samples using range-finder OSL dating. Quat. Geochron. 25, 1–9.
Lü, T., Sun, J., Li, S., Gong, Z., Xue, L., 2014. Vertical variations of luminescence sensitivity of quartz grains from loess/paleosol of Luochuan section in the central Chinese Loess Plateau since the last interglacial. Quat. Geochron. 22, 107–115.
Medlin, W.L., 1964. Trapping centres in thermoluminescent calcite. Phys. Rev. 135, A1770.
Munyikwa, K., Brown, S., 2014. Rapid equivalent dose estimation for eolian dune sands using a portable OSL reader and polymineralic standardised luminescence growth curves: expedited sample screening for OSL dating. Quat. Geochron. 22, 116–125.
Munyikwa, K., Kinnaird, T.C., Sanderson, D.C.W., 2021. The potential of portable luminescence readers in geomorphological investigations: a review. Earth Surf. Process. Landf. 46, 131–150.
Nitundil, S., Stone, A., Srivastava, A., 2023. Applicability of using portable luminescence reader for r 1 apid age-assessments of dune accumulation in the Thar Desert, India. Quat. Geochron., 101468
Pietsch, T.J., Olley, J.M., Nanson, G.C., 2008. Fluvial transport as natural luminescence sensitiser of quartz. Quat. Geochron. 41, 70–81.
Porat, N., Lopez, G.I., Lensky, N., Elinson, R., Avni, Y., Elgart-Sharon, Y., Faershtein, G., Gadot, Y., 2019. Using portable OSL reader to obtain a time scale for soil accumulation and erosion in archaeological terraces, the Judean Highlands, Israel. Quat. Geochron. 49, 65–70.
Rengers, F.K., Pagonis, V., Mahan, S.A., 2017. Can thermoluminescence be used to determine soil heating from a wildfire? Radiat. Meas. 107, 119–127. https://doi.org/10.1016/j.radmeas.2017.09.002.
Roberts, H.M., Duller, G.A.T., 2004. Standardised growth curve for optical dating of sediment using multiple-grain aliquots. Radiat. Meas. 38, 241–252.
Roberts, H.M., Durcan, J.A., Duller, G.A.T., 2009. Exploring procedures for the rapid assessment of optically stimulated luminescence range-finder ages. Radiat. Meas. 44, 582–587.
Sanderson, D.C.W., Chambers, D.A., 1985. An automatic 90-Sr irradiator for TL dating. Ancient TL 3, 26–29.
Sanderson, D.C.W., Murphy, S., 2010. Using simple portable OSL measurements and laboratory characterisation to help understand complex and heterogeneous sediment sequences for luminescence dating. Quat. Geochron. 5, 299–305.
Sanderson, D.C.W., Bishop, P., Houston, I., Boonsener, N., 2001. Luminescence characterisation of quartz rich cover sands from NE Thailand. Quat. Sci. Rev. 20, 893–900.
Sanderson, D.C.W., Bishop, P., Stark, M.T., Spencer, J.Q., 2003. Luminescence dating of anthropogenically reset canal sediments from Angkor Borei, Mekong Delta, Cambodia. Quat. Sci. Rev. 22, 1111–1121.
Sawakuchi, A.O., Blair, M.W., DeWitt, M.W., Faleiros, F.M., Hyppolito, T., Guedes, C.C. F., 2011. Thermal history versus sedimentary history: OSL sensitivity of quartz grains extracted from rocks and sediments. Quat. Geochron. 6, 261–272.
Schmidt, C., Halter, T., Hanson, P.R., Ulianov, A., Putlitz, B., King, G.E., Kreutzer, S., 2024. Zircon luminescence dating revisited. GChron. https://doi.org/10.5194/gchron-2024-10.
Stone, A., 2021. Dryland dunes and other dryland environmental archives as proxies for Late Quaternary stratigraphy and environmental and climate change in southern Africa. S. Afr. J. Geol. 124 (4), 927–962.
Stone, A., Fenn, K., 2022. Dating aeolian deposits. In: Shroder, J.J.F. (Ed.), Treatise on Geomorphology, vol. 7. Elsevier, Academic Press, pp. 120–168.
Stone, A., Bateman, M.D., Thomas, D.S.G., 2015. Rapid age assessment in the Namib Sand Sea using a portable luminescence reader. Quat. Geochron. 30, 134–140.
Stone, A., Bateman, M.D., Burrough, S.L., Garzanti, E., Limonta, M., Radeff, G., Telfer, M. W., 2019. Using a portable luminescence reader for rapid age assessment of aeolian sediments for reconstructing dunefield landscape evolution in southern Africa. Quat. Geochron. 49, 57–64.
Stone, A., Leader, G., Stratford, D., Marks, T., Efraim, K., Bynoe, R., Smedley, R., Gunn, A., Marais, E., 2024. Landscape evolution and hydrology at the Late Pleistocene archaeological site of Narabeb in the Namib Sand Sea, Namibia. Quat. Sci. Adv. 14, 100190. https://doi.org/10.1016/j.qsa.2024.100190.
Telfer, M.A., Bateman, M.D., Carr, A.S., Chase, B.M., 2008. Testing the applicability of a standardized growth curve (SGC) for quartz OSL dating: Kalahari dunes, South African coastal dunes and Florida dune cordons. Quat. Geochron. 3, 137–142.
Thomas, D.S.G., Burrough, S.L., 2012. Interpreting geoproxies of late Quaternary climate change in African drylands: implications for understanding environmental change and early human behaviour. Quat. Int. 253, 5–17.
Thomsen, K.J., Murray, A., Jain, M., Buylaert, J.-P., 2012. Re 'Luminescence dating of K-feldspar from sediments: a protocol without anomalous fading correction' by Bo Li and Sheng-Hua Li. Quat. Geochronol. 8, 46–48.

Wintle, A.G., Murray, A.S., 2006. A review of quartz optically stimulated luminescence characteristics and their relevance in single-aliquot regeneration dating protocols. Radiat. Meas. 41, 369–391.

Yang, L., Lai, Z., Long, H., Zhang, J., 2011. Construction of a quartz OSL standardised growth curve (SGC) for aeolian samples from the Horqin dunefield in northeastern China. Geochronometria 34 (4), 391–396.

Zheng, C.X., Zhouo, L.P., Qin, J.T., 2009. Difference in luminescence sensitivity of coarse-grained quartz from deserts of northern China. Radiat. Meas. 44 (5–6), 534–537.